Asian Journal of Chemistry; Vol. 33, No. 9 (2021), 2135-2142

ASIAN JOURNAL OF CHEMISTRY

https://doi.org/10.14233/ajchem.2021.23299

Thermal and Mechanical Properties of Flexible Poly(L-lactide)-*b*-polyethylene Glycol-*b*-poly(L-lactide)/Microcrystalline Cellulose Biocomposites

JENJIRA JIRUM and YODTHONG BAIMARK*

Biodegradable Polymers Research Unit, Department of Chemistry and Center of Excellence for Innovation in Chemistry, Faculty of Science, Mahasarakham University, Mahasarakham 44150, Thailand

*Corresponding author: Fax: +66 43 754246; Tel: +66 43 754246; E-mail: yodthong.b@msu.ac.th

Received: 12 May 2021; *Accepted*: 28 June 2021; *Published online*: 20 August 2021; AJC-20475

In this work, flexible biocomposites were prepared through melt blending using flexible poly(L-lactide)-*b*-polyethylene glycol-*b*-poly(L-lactide) (PLLA-PEG-PLLA) as a matrix and microcrystalline cellulose (MCC) as a filler. The effects of the addition of MCC on the thermal, morphological and mechanical properties of PLLA-PEG-PLLA/MCC biocomposites were investigated compared to PLLA/MCC biocomposites. Thermal stability of both PLLA and PLLA-PEG-PLLA from thermogravimetric analysis (TGA) was improved by MCC blending. Scanning electron microscopy (SEM) of the biocomposites exhibited good phase compatibility between PLLA-PEG-PLLA matrix-MCC filler. From tensile tests, the stress and strain at break of the PLLA/MCC and PLLA-PEG-PLLA/MCC biocomposite films decreased while the Young's modulus increased as the MCC content increased. The strain at break of PLLA-based and PLLA-PEG-PLLA based biocomposite films containing 20 wt.% MCC were 2% and 162%, respectively. Thus, the PLLA-PEG-PLLA/MCC biocomposites have potential to be used as flexible bioplastics for packaging applications.

Keywords: Poly(lactic acid), Block copolymer, Microcrystalline cellulose, Biocomposites.

INTRODUCTION

Poly(L-lactic acid) or poly(L-lactide) (PLLA) is one of the most bio-based thermoplastics that has been widely investigated for use in daily life as a replacement of conventional petroleum-based thermoplastics because of its eco-friendly nature, biosourcing, biodegradability, good tensile strength and excellent processability [1,2]. Currently, PLLA is employed in many applications such as biomedical, tissue engineering, pharmaceutical and packaging fields [3-5]. However, low flexibility and relatively high cost of PLLA often limit its use for a wider range of applications [6-8].

Modifications of PLLA like plasticization [9] and block copolymerization [10] have been proposed to improve the flexibility of PLLA. The migration effect of plasticizers on aging can be neglected for block copolymerization. PLLA has been copolymerized with flexible polyethylene glycol (PEG) to obtain PLLA-*b*-PEG-*b*-PLLA triblock copolymers (PLLA-PEG-PLLA) which were more flexible and showed faster crystallization than PLLA due to the PEG middle-blocks enhancing chain mobility [11,12]. These PLLA-PEG-PLLA have potential for use as highly flexible bioplastics.

Microcrystalline cellulose (MCC) is a bio-filler for development of polymer-based composites. MCC showed low density, strong mechanical properties, high crystallinity, non-toxic, renewability, biodegradability and low cost when it was prepared by removing the amorphous phase of purified cellulosic fibers *via* acid hydrolysis [13,14]. It is widely used in food, medical, pharmaceutical, food, beverage and cosmetic industries [14]. Generally, used as a filler to prepare low cost PLLA-based biocomposites [15,16]. The addition of MCC decreased tensile stress and strain at break of PLLA whereas Young's modulus was increased. The PLLA/MCC biocomposites exhibited lower flexibility than the PLLA. However, the addition of MCC improved thermal stability of the PLLA [16].

To the best of our knowledge, there have not been any reports for the influence of MCC addition on the properties of flexible PLLA-PEG-PLLA bioplastics. Therefore, the objective of this work was to fabricate PLLA-PEG-PLLA/MCC biocomposites. The PLLA/MCC biocomposites were also prepared

for comparison. The thermal, morphological and mechanical properties of the obtained biocomposites were determined and discussed.

EXPERIMENTAL

Poly(L-lactic acid) (PLLA) and poly(L-lactide)-*b*-poly-ethylene glycol-*b*-poly(L-lactide) (PLLA-PEG-PLLA) were synthesized through ring-opening polymerization in bulk as described [12]. The PLLA and PLLA-PEG-PLLA with similar melt flow indices were used as the polymer matrices for preparing the biocomposites because they have similar melt flow properties during melt blending with MCC powder. Therefore, the non-chain-extended PLLA (MFI = 23 g/10 min) and chain-extended PLLA-PEG-PLLA with 4.0 phr Joncryl® ADR-4368 chain extender (MFI = 24 g/10 min) were chosen for this purpose [12]. The microcrystalline cellulose (MCC) powder with particle size less than 150 μm was obtained from Xi'an Sgonek Biological Technology Co., Ltd., China. It's degree of crystallinity was 79.3% as obtained from the XRD analysis. The morphology of MCC particles is shown in Fig. 1.

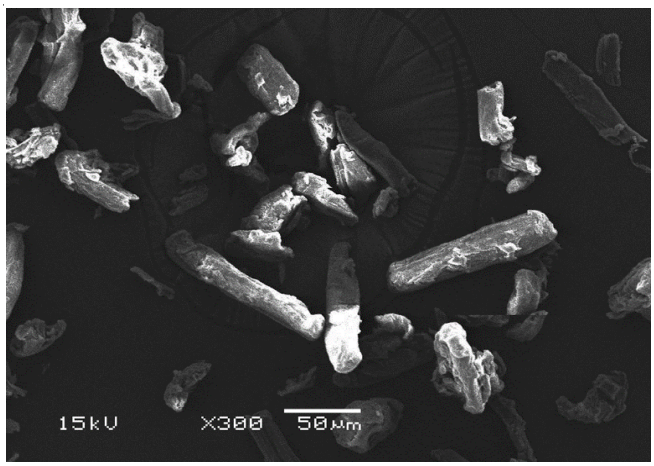

Fig. 1. SEM image of MCC particles (Bar scale = 50 μm)

Preparation of biocomposites and their films: PLLA-PEG-PLLA and MCC were dried *in vacuo* at 50 ºC overnight to remove moisture before melt blending with a Rheomix batch mixer (HAAKE Polylab OS). Melt blending was performed at 190 ºC for 4 min with a rotor speed of 100 rpm. The biocomposites with PLLA-PEG-PLLA/MCC ratios of 100/0, 95/5, 90/10 and 80/20 (w/w) were investigated. he PLLA/MCC biocomposites were prepared by the same method for comparison.

The biocomposites were dried *in vacuo* at 50 ºC overnight before film formed using a compression molding machine (Auto CH Carver). The biocomposites were heated at 200 ºC for 3.0 min without any force before compressing at 200 ºC for 1.0 min under 5.0 ton load. The obtained films were then quickly cooled to 25 ºC with water flow under 5.0 ton load for 1.0 min.

Characterization: Thermal transition properties of the biocomposites were determined using a differential scanning calorimeter (DSC, Perkin-Elmer Pyris Diamond) under the nitrogen gas atmosphere. The biocomposites were melted at 200 ºC for 3 min to remove their thermal history, then fast quenched before heating from 0 to 200 ºC at a rate of 10 ºC/min to observe glass transition (T_g), cold crystallization (T_{cc}) and melting (T_m) temperatures as well as enthalpies of melting (ΔH_m) and cold crystallization (ΔH_{cc}). The degree of crystallinity (X_c) of PLLA was calculated from the ΔH_m and ΔH_{cc} using eqn. 1:

$$X_c\ (\%) = \frac{\Delta H_m - \Delta H_{cc}}{93 \times W_{PLLA}} \times 100 \quad (1)$$

where, ΔH_m = 93 J/g for 100% X_c PLLA [17]. The W_{PLLA} is the PLLA weight-fraction of the biocomposites calculated from PLLA fraction (PLLA = 1.00 and PLLA-PEG-PLLA = 0.83 obtained from ^{1}H NMR) [12] and MCC = microcrystalline cellulose content.

To investigate crystallization behaviours, the biocomposites were melted at 200 ºC for 3 min to erase their thermal history before cooling from 200 to 0 ºC at a rate of 10 ºC/min to observe the crystallization temperature (T_c) and enthalpy of crystallization (ΔH_c).

Thermal stability of the biocomposites was determined using a thermogravimetric analyzer (TGA, TA-Instrument SDT Q600). TGA was carried out in the range of 50 to 800 ºC at a heating rate of 20 ºC/min under a nitrogen gas flow to prevent oxidative thermal decomposition.

The crystalline structures of the biocomposite films were investigated using a wide angle X-ray diffractometer (XRD, Bruker D8 Advance) in the angle range of 2θ = 5º-30º equipped with a copper tube operating at 40 kV and 40 mA producing Cu*K*α radiation and the scan speed was 3º per min.

The phase morphology of the biocomposite films was observed using a scanning electron microscope (SEM, JEOL JSM-6460LV). The biocomposite films were cryogenically fractured after immersing in liquid nitrogen and sputter coated with gold to avoid charging before scanning at an acceleration voltage of 15 kV.

The tensile properties of the biocomposite films were measured using an universal mechanical testing machine (Liyi Environmental Technology LY-1066B, China) with a load cell of 100 kg, a crosshead speed of 50 mm/min and a gauge length of 50 mm. The film sizes were 100 mm × 10 mm. The averaged tensile properties were obtained from at least five measurements.

RESULTS AND DISCUSSION

Thermal transition properties: The DSC has been extensively used to determine the thermal transition properties of PLLA-based composites [1,3,13]. The DSC heating curves of pure PLLA, pure PLLA-PEG-PLLA and their biocomposites are shown in Fig. 2 and DSC results are summarized in Table-1. It was found that the T_g for PLLA/MCC and PLLA-PEG-PLLA/MCC biocomposites were in ranges of 53-56 ºC and 33-34 ºC, respectively, indicating that the T_g was not significantly changed by the addition of MCC. However, the MCC blending caused significant shifting of T_{cc} to higher temperature for both the PLLA/MCC and PLLA-PEG-PLLA/MCC biocomposite series. This indicates that the MCC blending inhibited PLLA crystallization. According to the literature, it

TABLE-1
THERMAL TRANSITION PROPERTIES OF PLLA/MCC AND PLLA-PEG-PLLA/MCC BIOCOMPOSITES FROM DSC HEATING CURVES

Biocomposites	PLLA/MCC (w/w)						PLLA-PEG-PLLA/MCC (w/w)					
	T_g (°C)	T_{cc} (°C)	ΔH_{cc} (J/g)	T_m (°C)	ΔH_m (J/g)	X_c (%)	T_g (°C)	T_{cc} (°C)	ΔH_{cc} (J/g)	T_m (°C)	ΔH_m (J/g)	X_c (%)
100/0	53	92	19.5	174	42.3	24.3	34	65	7.0	169	42.9	46.2
95/5	56	98	22.0	174	35.9	15.6	33	76	16.8	170	43.7	36.4
90/10	54	100	24.3	174	36.0	13.9	34	78	19.1	169	43.4	34.7
80/20	54	102	27.4	173	36.3	11.9	33	77	19.0	168	39.2	32.5

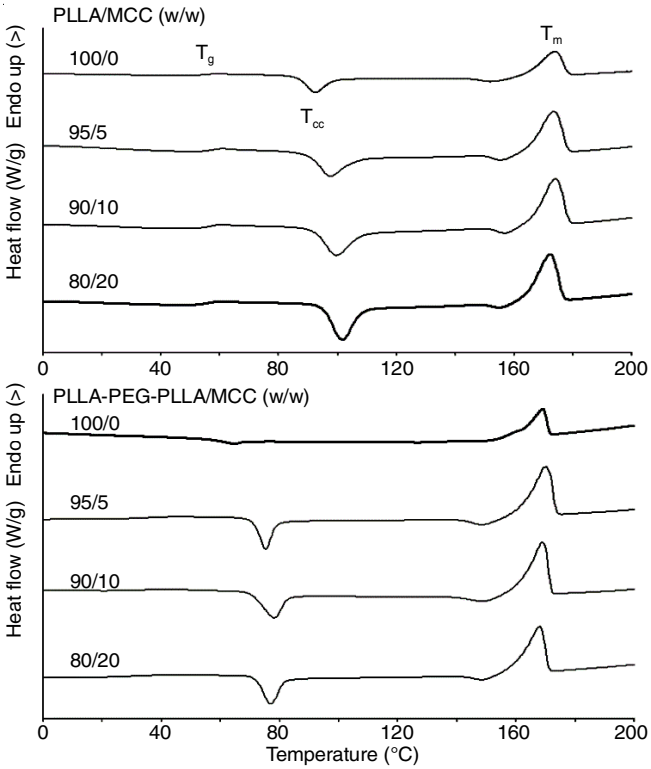

Fig. 2. DSC heating curves of (above) PLLA/MCC and (below) PLLA-PEG-PLLA/MCC biocomposites with various MCC contents

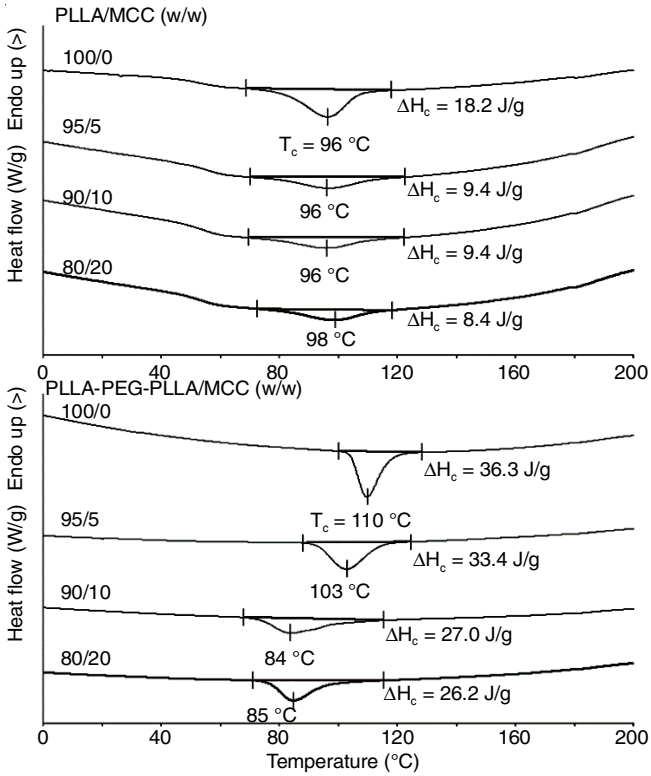

Fig. 3. DSC cooling curves of (above) PLLA/MCC and (below) PLLA-PEG-PLLA/MCC biocomposites with various MCC contents

has been reported that MCC in the PLLA/MCC biocomposites restricted chain mobility for PLLA crystallization [16]. Therefore, the X_c of both PLLA/MCC and PLLA-PEG-PLLA/MCC biocomposites steadily decreased as the MCC content increased as reported in Table-1. It should be noted that all the PLLA-PEG-PLLA/MCC biocomposites had lower T_{cc} and larger X_c than the PLLA/MCC. The results suggested that the crystallizability of PLLA-PEG-PLLA/MCC biocomposites was better due to the flexible PEG middle-blocks of PLLA-PEG-PLLA enhanced chain mobility for crystallization of PLLA end-blocks [11,12].

DSC cooling scans were also carried out as presented in Fig. 3 to show the T_c and ΔH_c behaviour of the biocomposites. The PLLA/MCC biocomposites did not obviously change their T_c with changed MCC content while the T_c of PLLA-PEG-PLLA/MCC biocomposites dramatically shifted to lower temperature as the MCC content increased. However, the ΔH_c for both PLLA/MCC and PLLA-PEG-PLLA/MCC biocomposites significantly decreased with increasing MCC content. The results of T_c and ΔH_c clearly supported that the MCC blending suppressed the PLLA crystallization of biocomposites.

Thermal stability: Thermal stability of the biocomposites is important information on the processing window for melt processing that was investigated from thermograms as shown in Fig. 4. Pure PLLA and MCC exhibited a single thermal decomposition step at 300-450 ºC (Fig. 4 (above)] and 250-500 ºC (TG curve not shown), respectively. The PLLA/MCC biocomposites exhibited only a single thermal-decomposition step in the range 300-450 ºC (Fig. 4). The decomposition temperatures for 50% weight remaining (50%-T_d) of the PLLA and PLLA/MCC biocomposites slightly shifted to higher temperature as the MCC content increased as summarized in Table-2.

Thermogravimetric curves of pure PLLA-PEG-PLLA are shown in Fig. 4 (below) indicating that it had two thermal-decomposition steps in ranges 250-350 ºC and 350-450 ºC attributed to thermal decompositions for PLLA and PEG blocks, respectively [12,18]. The 50%-T_d of all the PLLA-PEG-PLLA/MCC biocomposites in Table-2 were higher than the pure PLLA-PEG-PLLA, which is largely shifted to higher temperature as the MCC content increased. The results suggested that the MCC blending improved the thermal stability of both PLLA and PLLA-PEG-PLLA biocomposites.

TABLE-2
THERMAL DECOMPOSITION PROPERTIES OF PLLA/MCC AND PLLA-PEG-PLLA/MCC BIOCOMPOSITES

Biocomposites	PLLA/MCC (w/w)					PLLA-PEG-PLLA/MCC (w/w)				
	50%-T_d (°C)[a]	Residue weight at 800 °C (%)[a]	PLLA-$T_{d,max}$ (°C)[b]	MCC-$T_{d,max}$ (°C)[b]	PEG-$T_{d,max}$ (°C)[b]	50%-T_d (°C)[a]	Residue weight at 800 °C (%)[a]	PLLA-$T_{d,max}$ (°C)[b]	MCC-$T_{d,max}$ (°C)[b]	PEG-$T_{d,max}$ (°C)[b]
100/0	352	0.03	362	–	–	309	0.11	310	–	417
95/5	353	0.61	363	–	–	313	0.52	314	–	413
90/10	357	1.39	366	–	–	321	1.30	321	366	418
80/20	359	2.55	366	–	–	331	2.95	326	367	419

[a]Obtained from TG thermograms; [b]Obtained from DTG thermograms

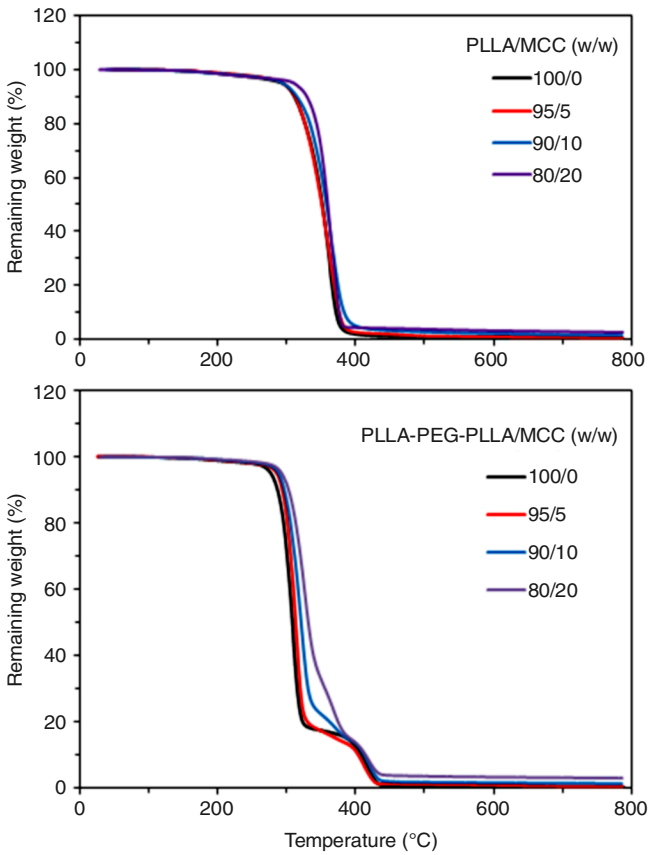

Fig. 4. TG thermograms of (above) PLLA/MCC and (below) PLLA-PEG-PLLA/MCC biocomposites with various MCC contents

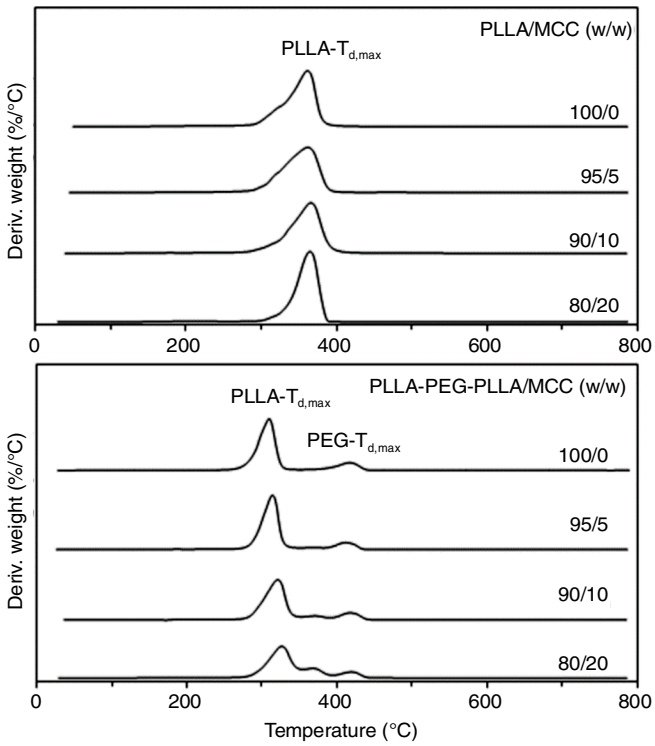

Fig. 5. DTG thermograms of (above) PLLA/MCC and (below) PLLA-PEG-PLLA/MCC biocomposites with various MCC contents

The weight residues at 800 ºC for PLLA, PLLA-PEG-PLLA and MCC were 0.05%, 0.11% and 7.64%, respectively. The residue weights at 800 ºC for both the PLLA/MCC and PLLA-PEG-PLLA/MCC biocomposite series increased steadily with the MCC content as reported in Table-2 due to the increase of MCC ashes.

Derivative TG (DTG) thermograms in Fig. 5 gave more information on thermal decomposition of the biocomposites. The peak for temperature of maximum decomposition-rate ($T_{d,max}$) was detected from their DTG thermograms. The $T_{d,max}$ results are also summarized in Table-2. The $T_{d,max}$ of pure PLLA (PLLA-$T_{d,max}$) had only one peak at 362 ºC assigned to PLLA decomposition. The $T_{d,max}$ of PLLA/MCC biocomposites was slightly shifted to higher temperature with the MCC content. The $T_{d,max}$ peak of MCC was 357 ºC (DTG curve not shown) may be overlapped with the PLLA-$T_{d,max}$ peak.

While the pure PLLA-PEG-PLLA exhibited two $T_{d,max}$ peaks at 310 and 417 ºC attributed to decomposition of PLLA (PLLA-$T_{d,max}$) and PEG (PEG-$T_{d,max}$), respectively. The PLLA-$T_{d,max}$ of PLLA-PEG-PLLA/MCC biocomposites steadily shifted to higher temperature with increasing MCC content as reported in Table-2. The results supported the interpretation that the MCC blending improved thermal stability for the PLLA-PEG-PLLA more than the PLLA. This may be explained by the stronger interactions between the PLLA-PEG-PLLA and MCC components. The PLLA-PEG-PLLA was more hydrophilic than PLLA due to the hydrophilic characters of PEG middle-blocks [19]. This may be supported by the observation that MCC-$T_{d,max}$ increased from 357 to 366 ºC and 367 ºC for the 90/10 and 80/20 PLLA-PEG-PLLA/MCC biocomposites, respectively as reported in Table-2.

Crystalline structure: The XRD pattern of the biocomposite films was used to study their crystalline structures as shown in Fig. 6. The pure PLLA and PLLA/MCC biocomposite films in Fig. 6(above) had no XRD peaks attributable to the

PLLA crystallites at 2θ = 15º, 17º and 19º [12,18]. This indicates the PLLA matrices had completely amorphous characters. The pure PLLA-PEG-PLLA film in Fig. 6(below) exhibited only one XRD peak at 2θ = 17º attributed to PLLA crystallites due to the flexible PEG middle-blocks of PLLA-PEG-PLLA which enhanced the crystallization of PLLA end-blocks [11,12]. However, the intensity of this XRD peak decreased and disappeared when 5 wt.% MCC was blended and the MCC content was increased up to 10 wt.%. The MCC blending suppressed the crystallization of the PLLA end-blocks.

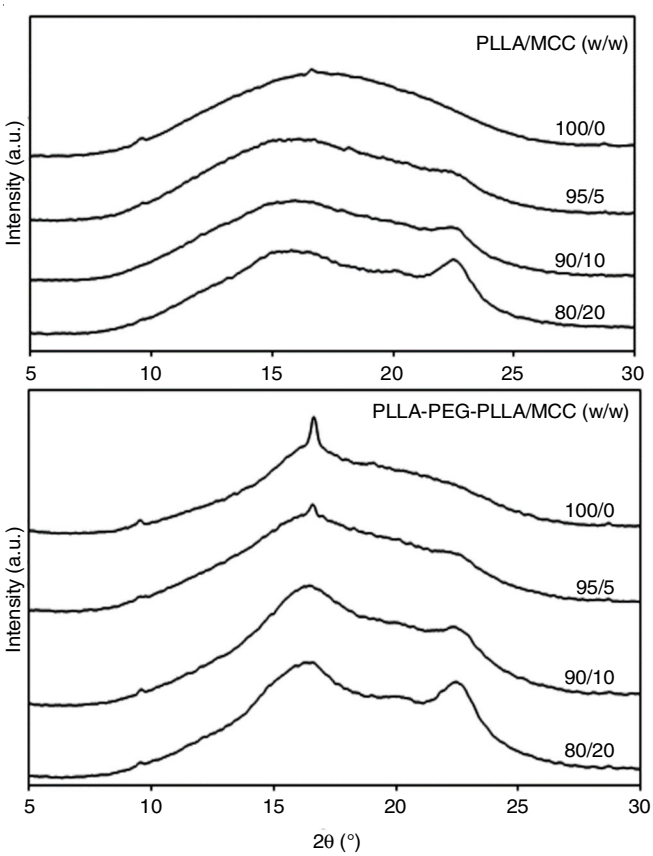

Fig. 6. XRD patterns of (above) PLLA/MCC and (below) PLLA-PEG-PLLA/MCC biocomposite films with various MCC contents

It should be noted that the XRD peaks of cellulose crystallites for MCC were also observed at 2θ = 22.5º for all the PLLA/MCC and PLLA-PEG-PLLA/MCC biocomposite films [15,20]. The intensity of the XRD peak at 2θ = 22.5º steadily increased as the MCC content increased indicating that biocomposite films with different MCC contents could be prepared.

Film morphology: SEM images of cryo-fractured films were usually observed to investigate phase separation and phase compatibility between film matrix and MCC particles. Fig. 7 shows SEM images of both pure PLLA and pure PLLA-PEG-PLLA films. The cross-section of the PLLA film from brittle fracture was smoother than that of the PLLA-PEG-PLLA film. This was due to the higher T_g and lower flexibility of the PLLA film compared with the PLLA-PEG-PLLA film while the film matrices of PLLA-PEG-PLLA were extended before fracture and could be demonstrated as ductile fracture [12].

SEM images of 20 wt.% MCC biocomposite films are clearly compared in Fig. 8 with different magnifications. The phase separation between the film matrices and MCC particles was visibly observed. However, gaps between PLLA matrices and MCC particle surfaces can also be easily observed (Fig. 8b). Moreover, some irregular cavities from MCC particles falling out of the fractured surfaces were also detected. This can be explained by the different in hydrophilicity between PLLA and MCC [21]. While the PLLA-PEG-PLLA/MCC biocomposite films showed good interfacial adhesion between film matrices and MCC particles (Fig. 8d). PEG has been used as a compatibilizer to induce interfacial adhesive between PLLA and cellulose particles [22]. Thus, this can be explained as that the hydrophilic PEG middle-blocks enhanced phase compatibility between PLLA-PEG-PLLA and MCC.

Tensile properties: Typical tensile curves of the biocomposite films are shown in Fig. 9. Strain at break for all the PLLA-PEG-PLLA/MCC biocomposite films in Fig. 9 (below) were largely higher than the PLLA/MCC biocomposite films in Fig. 9 (above). Moreover, all the PLLA-PEG-PLLA/MCC biocomposite films also exhibited a yield point. The results indicated that all the PLLA-PEG-PLLA/MCC biocomposite films were more extensible than those of the PLLA/MCC bio-

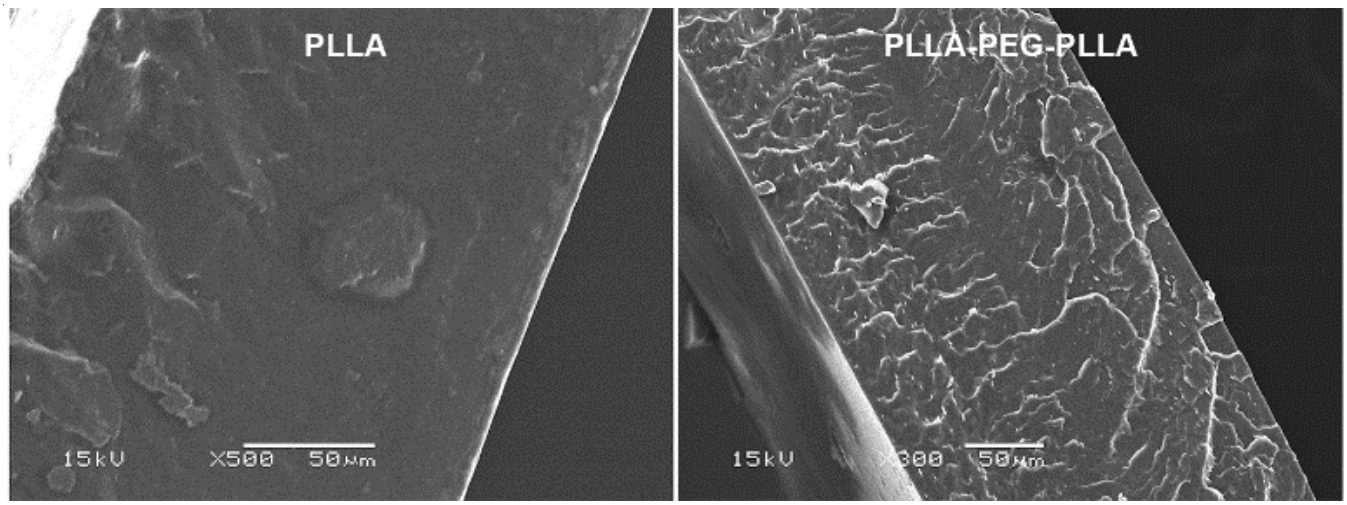

Fig. 7. SEM images of cryo-fractured of (left) pure PLLA and (right) pure PLLA-PEG-PLLA films (Both bar scales = 50 µm)

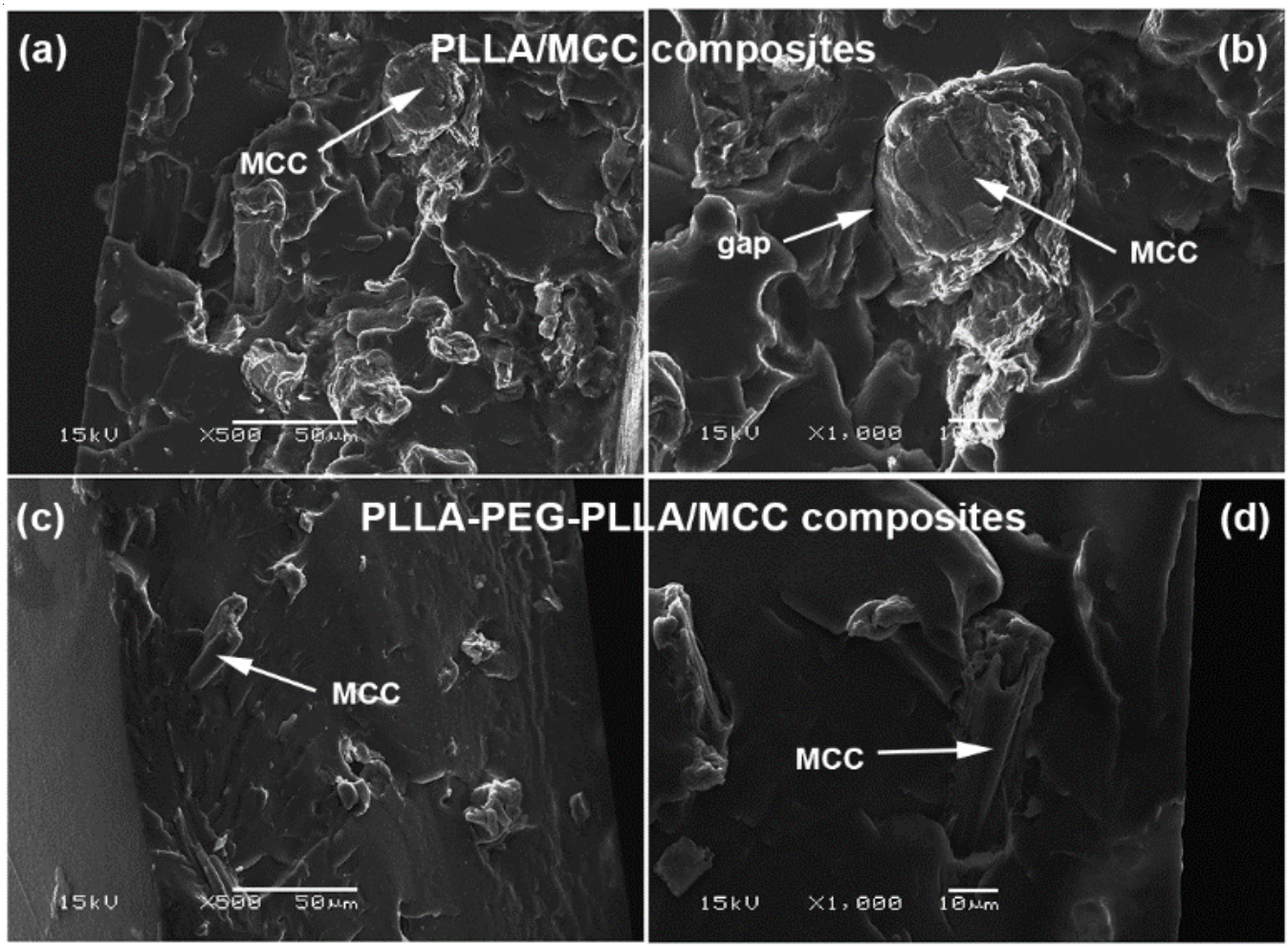

Fig. 8. SEM images of cryo-fractured of (a, b) 80/20 (w/w) PLLA/MCC and (c, d) 80/20 (w/w) PLLA-PEG-PLLA/MCC biocomposite films (Bar scales = 50 µm for a, c and = 10 µm for b, d)

composite films. The flexible PEG middle-blocks enhanced extensibility of PLLA-PEG-PLLA/MCC biocomposite films [12,18]. The averaged tensile properties are summarized in Table-3.

The stress and strain at break of both PLLA and PLLA-PEG-PLLA films decreased steadily when the MCC was blended at increasing content. The stress at yield of the PLLA-PEG-PLLA/MCC biocomposite films also decreased as the MCC content increased but the strain at yield did not change in trend. The agglomeration of MCC and poor matrix-MCC adhesion caused decreases of stress and strain at break of the biocomposite films [3,16]. The results indicated that the interfacial adhesion on PLLA-PEG-PLLA/MCC biocomposites was not strong enough for enhancing stress transfer from PLLA-PEG-PLLA matrix to the MCC particle surfaces to improve the stress at break of the biocomposite films. Young's modulus of the biocomposite films increased with the MCC content. This is due to the high crystallinity of MCC inducing an increase of the Young's modulus of the biocomposite films [16].

However, from results of tensile properties, the PLLA-PEG-PLLA/MCC biocomposites still exhibited higher flexibility than those of the PLLA/MCC biocomposites for all the MCC contents.

Film transparency: Packaging films with good transparency are interesting because they enable the quality and quantity of the packed products to be directly observed. Figs.

TABLE-3
AVERAGED TENSILE PROPERTIES OF PLLA/MCC AND PLLA-PEG-PLLA/MCC BIOCOMPOSITE FILMS

Biocomposite films	PLLA/MCC (w/w)					PLLA-PEG-PLLA/MCC (w/w)				
	Stress at yield (MPa)	Strain at yield (%)	Stress at break (MPa)	Strain at break (%)	Young's modulus (MPa)	Stress at yield (MPa)	Strain at yield (%)	Stress at break (MPa)	Strain at break (%)	Young's modulus (MPa)
100/0	–	–	43.9±3.1	4.2±0.6	1466±101	15.6±3.2	4.9±1.2	19.9±1.4	374.6±43.0	672±63
95/5	–	–	41.3±4.1	3.3±0.2	1530±92	11.3±1.1	4.3±0.9	15.6±1.0	255.0±21.5	696±54
90/10	–	–	37.1±2.1	3.2±0.1	1559±89	11.1±2.4	4.9±1.4	15.1±0.5	224.6±9.8	726±78
80/20	–	–	31.5±1.6	2.0±0.2	1749±104	10.2±2.8	4.6±1.5	12.2±0.5	161.5±13.9	798±68

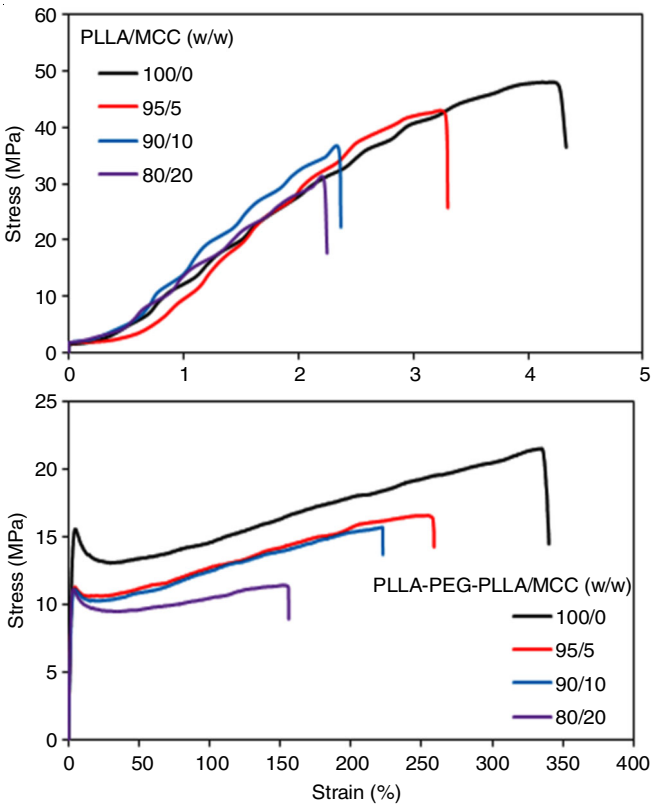

Fig. 9. Tensile curves of (above) PLLA/MCC and (below) PLLA-PEG-PLLA/MCC biocomposite films with various MCC contents.

10 and 11 show the film transparency of PLLA/MCC and PLLA-PEG-PLLA/MCC biocomposite films, respectively. They had good transparency and with increasing MCC loading, film transparency slightly decreased.

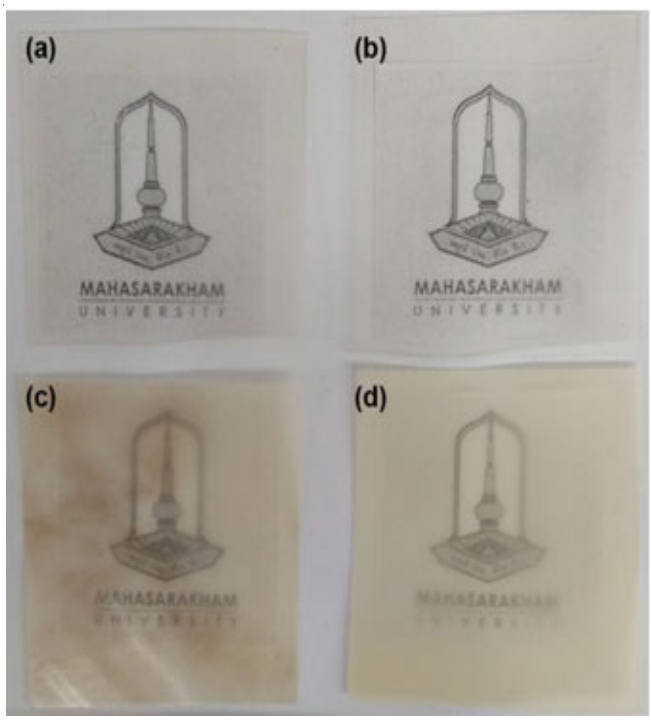

Fig. 10. Film transparency of PLLA films (a) without MCC and with MCC contents of (b) 5, (c) 10 and (d) 20 wt.%

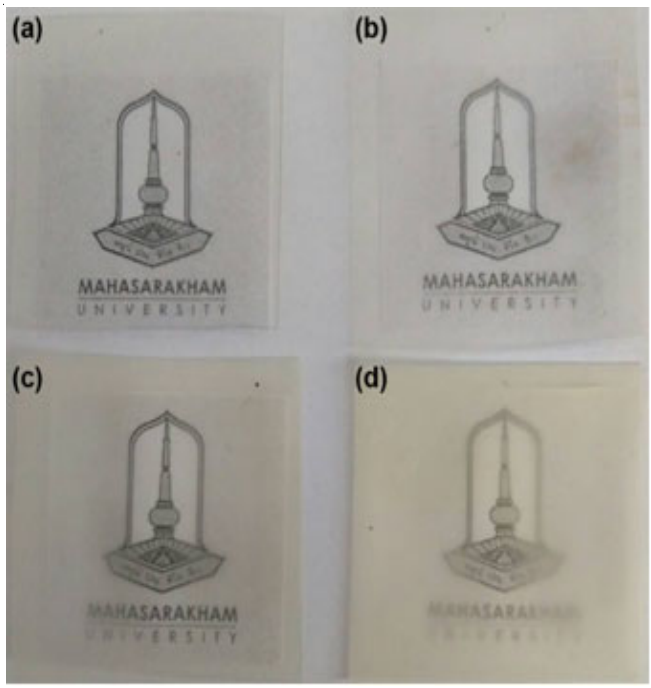

Fig. 11. Film transparency of PLLA-PEG-PLLA films (a) without MCC and with MCC contents of (b) 5, (c) 10 and (d) 20 wt.%

Some agglomeration of MCC particles due to the filler-filler interactions [23] was observed for the PLLA/MCC biocomposite films as the MCC content increased up to 10 wt.% but was not observed for the PLLA-PEG-PLLA/MCC biocomposite films. The results of the film transparency supported the that the phase compatibility of PLLA-PEG-PLLA/MCC biocomposites is better than the PLLA/MCC biocomposites.

Conclusion

The PLLA/MCC and PLLA-PEG-PLLA/MCC biocomposites were obtained successfully by melt blending technique. The DSC and XRD studies indicated that the MCC addition suppressed PLA crystallization. The X_c of PLLA decreased significantly with the increasing MCC content. The addition of MCC in both the PLLA and PLLA-PEG-PLLA matrix improved the thermal stability of the biocomposites as revealed by the TGA results. The PLLA-$T_{d,max}$ of both PLLA/MCC and PLLA-PEG-PLLA/MCC biocomposites shifted to a higher temperature when the MCC content was increased. The hydrophilic PEG middle-blocks enhanced phase compatibility between the PLLA-PEG-PLLA matrix and MCC filler as observed from SEM images. Tensile properties of both PLLA/MCC and PLLA-PEG-PLLA/MCC biocomposite films indicated that the stress and strain at break decreased with increasing MCC content due to poor interfacial adhesion between film matrix-MCC filler. Young's modulus increased as the MCC content increased due to high crystallinity of MCC. The PLLA-PEG-PLLA/MCC biocomposite films displayed a higher flexibility as compared to PLLA/MCC biocomposite films. The extensibility of PLLA-PEG-PLLA-based biocomposites can be tailored by selecting the appropriate MCC content. Thus, the PLLA-PEG-PLLA/MCC biocomposites could be appropriate for use as flexible biodegradable biocomposites in packaging applications.

ACKNOWLEDGEMENTS

The authors acknowledge Mahasarakham University for providing the research faciliteis. The authors also thank the Center of Excellence for Innovation in Chemistry (PERCH-CIC), Office of the Higher Education Commission, Ministry of Education, Thailand for conducting the tensile test studies.

CONFLICT OF INTEREST

The authors declare that there is no conflict of interests regarding the publication of this article.

REFERENCES

1. K. Hamad, M. Kaseem, M. Ayyoob, J. Joo and F. Deri, *Prog. Polym. Sci.*, **85**, 83 (2018); https://doi.org/10.1016/j.progpolymsci.2018.07.001
2. V.H. Sangeetha, H. Deka, T.O. Varghese and S.K. Nayak, *Polym. Compos.*, **39**, 81 (2018); https://doi.org/10.1002/pc.23906
3. D. da Silva, M. Kaduri, M. Poley, O. Adir, N. Krinsky, J. Shainsky-Roitman and A. Schroeder, *Chem. Eng. J.*, **340**, 9 (2018); https://doi.org/10.1016/j.cej.2018.01.010
4. V. DeStefano, S. Khan and A. Tabada, *Eng. Regener.*, **1**, 76 (2020); https://doi.org/10.1016/j.engreg.2020.08.002
5. S. Liu, S. Qin, M. He, D. Zhou, Q. Qin and H. Wang, *Compos. B Eng.*, **199**, 108238 (2020); https://doi.org/10.1016/j.compositesb.2020.108238
6. L. Quiles-Carrillo, M.M. Blanes-Martinez, N. Montanes, O. Fenollar, S. Torres-Giner and R. Balart, *Eur. Polym. J.*, **98**, 402 (2018); https://doi.org/10.1016/j.eurpolymj.2017.11.039
7. F.L. Jin, R.R. Hu and S.J. Park, *Composite B Eng.*, **164**, 287 (2019); https://doi.org/10.1016/j.compositesb.2018.10.078
8. B. Wang, Y. Jin, K. Kang, N. Yang, Y. Weng, Z. Huang and S. Men, *E-Polymers*, **20**, 39 (2020); https://doi.org/10.1515/epoly-2020-0005
9. M. Baiardo, G. Frisoni, M. Scandola, M. Rimelen, D. Lips, K. Ruffieux and E. Wintermantel, *J. Appl. Polym. Sci.*, **90**, 1731 (2003); https://doi.org/10.1002/app.12549
10. S. Farah, D.G. Anderson and R. Langer, *Adv. Drug Deliv. Rev.*, **107**, 367 (2016); https://doi.org/10.1016/j.addr.2016.06.012
11. X. Yun, X. Li, Y. Jin, W. Sun and T. Dong, *Polym. Sci. Ser. A*, **60**, 141 (2018); https://doi.org/10.1134/S0965545X18020141
12. Y. Baimark, W. Rungseesantivanon and N. Prakymoramas, *Mater. Des.*, **154**, 73 (2018); https://doi.org/10.1016/j.matdes.2018.05.028
13. M. Murariu and P. Dubois, *Adv. Drug Deliv. Rev.*, **107**, 17 (2016); https://doi.org/10.1016/j.addr.2016.04.003
14. D. Trache, M.H. Hussin, C.T. Hui Chuin, S. Sabar, M.R.N. Fazita, O.F.A. Taiwo, T.M. Hassan and M.K.M. Haafiz, *Int. J. Biol. Macromol.*, **93**, 789 (2016); https://doi.org/10.1016/j.ijbiomac.2016.09.056
15. A.P. Mathew, K. Oksman and M. Sain, *J. Appl. Polym. Sci.*, **97**, 2014 (2005); https://doi.org/10.1002/app.21779
16. M.K.M. Haafiz, A. Hassan, Z. Zakaria, I.M. Inuwa, M.S. Islam and M. Jawaid, *Carbohydr. Polym.*, **98**, 139 (2013); https://doi.org/10.1016/j.carbpol.2013.05.069
17. F.A. Syamani, Y.D. Kurniawan and L. Suryanegara, *Asian J. Chem.*, **30**, 1435 (2018); https://doi.org/10.14233/ajchem.2018.21119
18. Y. Baimark and Y. Srisuwan, *J. Elastomers Plast.*, **52**, 142 (2020); https://doi.org/10.1177/0095244319827993
19. Y. Baimark, S. Pasee, W. Rungseesan and N. Prakymoram, *Asian J. Sci. Res.*, **12**, 508 (2019); https://doi.org/10.3923/ajsr.2019.508.515
20. M. Hasan, T.K. Lai, D.A. Gopakumar, M. Jawaid, F.A.T. Owolabi, E.M. Mistar, T. Alfatah, N.Z. Noriman, M.K.M. Haafiz and H.P.S. Abdul Khalil, *J. Polym. Environ.*, **27**, 1602 (2019); https://doi.org/10.1007/s10924-019-01457-4
21. X. Dai, Z. Xiong, H. Na and J. Zhu, *Compos. Sci. Technol.*, **90**, 9 (2014); https://doi.org/10.1016/j.compscitech.2013.10.009
22. P. Qu, Y. Gao, G.F. Wu and L.P. Zhang, *BioResources*, **5**, 1811 (2010).
23. G.H. Yew, A.M. Mohd Yusof, Z.A. Mohd Ishak and U.S. Ishiaku, *Polym. Degrad. Stabil.*, **90**, 488 (2005); https://doi.org/10.1016/j.polymdegradstab.2005.04.006